EXPERIMENTAL VERIFICATION OF EDDY-CURRENT FLAW THEORY*

C. V. Dodd, C. D. Cox,† and W. E. Deeds‡

Metals and Ceramics Division
Oak Ridge National Laboratory
Oak Ridge, Tennessee 37831

INTRODUCTION

Carefully machined flaw samples in plates and tubes were examined with eddy-current coils of accurately known dimensions. Both near- and far-side flaws were measured using absolute and differential coil modes. The experimental data were compared with computer calculations based on the flaw theory of Burrows and the analytical solutions of Dodd and Deeds. The experimental and theoretical data are in good agreement whenever the flaw size is small compared to the other significant dimensions, but large enough to give a reasonable signal-to-noise ratio for the measuring instrument. The experimental and analytical readings are also used to check our flaw inversion theory.

EXPERIMENTAL MEASUREMENTS

As part of a long-term program to verify the accuracy of analytical solutions[1-3] to eddy-current problems and the infinitesimal flaw theory of Burrows,[4] we have made accurate measurements of the impedance changes as accurately made coils are scanned past accurately machined flaws in aluminum plates and tubes.

In order to minimize experimental errors, the coils and samples were rather large, and the measurements were made with a Hewlett-Packard 4192A low-frequency impedance analyzer and 16095A probe fixture

---

*Research sponsored by the Office of Nuclear Regulatory Research, U.S. Nuclear Regulatory Commission, under Interagency Agreement DOE 40-551-75 with the U.S. Department of Energy under contract DE-AC05-840R21400 with Martin Marietta Energy Systems, Inc.

†Oak Ridge Associated Universities Summer Undergraduate Research Participant.

‡Adjunct Research Participant, The University of Tennessee, Knoxville.

at a frequency of 400 Hz. The 6061-T6 aluminum tube and plate were 6.35 mm thick (0.250 in.), and the inner diameter of the tube was 76 mm (3.00 in.). The machined flaws were flat-bottom holes in the outer surface of the tube and in one side of the plate; the depth of each hole was approximately equal to its diameter. Accurately dimensioned coils were made to fit inside and outside the tube, so that both far- and near-side measurements could be made with the tube as well as the plate. Eddy-current measurements were made with coils in both absolute and differential modes as coils were scanned past the flaws (see Fig. 1).

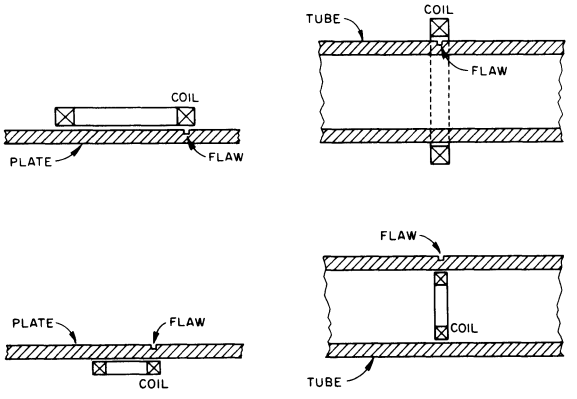

Fig. 1. Experimental arrangements of coil, conductor, and flaw.

Figures 2 and 3 show calculated and experimental values of the normalized impedance changes as a coil is scanned past a flaw in a flat plate; the flaw dimensions are shown in the figures. The calculated points were obtained by computer using the Burrows small-flaw theory with analytical solutions for the vector potential to calculate the coil impedance changes produced by a small flaw of known size and location in a medium of known resistivity.

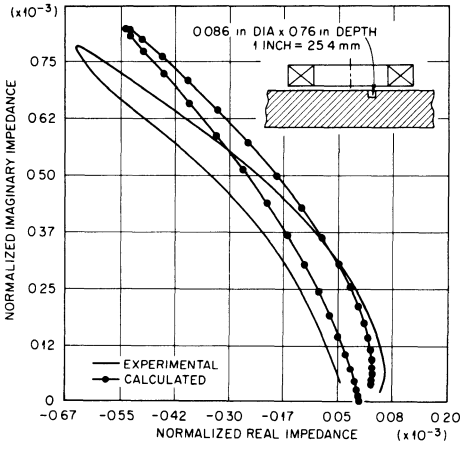

Fig. 2. Near-side flaw in a plate.

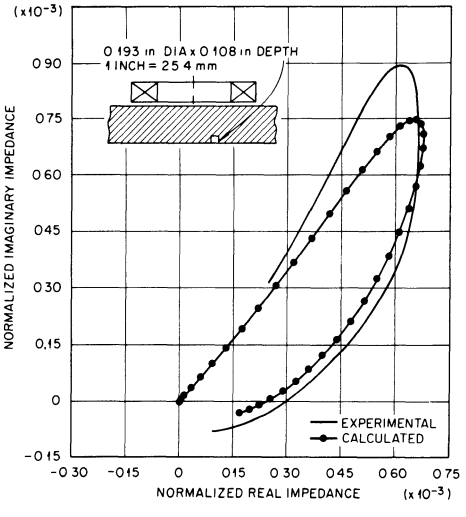

Fig. 3. Far-side flaw in a plate.

Figures 4, 5, and 6 show similar normalized impedance changes for coils scanned past a flaw in a tube; the coil arrangement and flaw dimensions are shown in each figure.

In general, the agreement between calculated and experimental measurements was reasonably good whenever the flaw was large enough to produce a reasonable signal change, but not so large that its dimensions were comparable to the wall thickness or the skin depth. In the latter case, the assumption that the induced eddy-current density would have been constant throughout the defect region is definitely not satisfied.

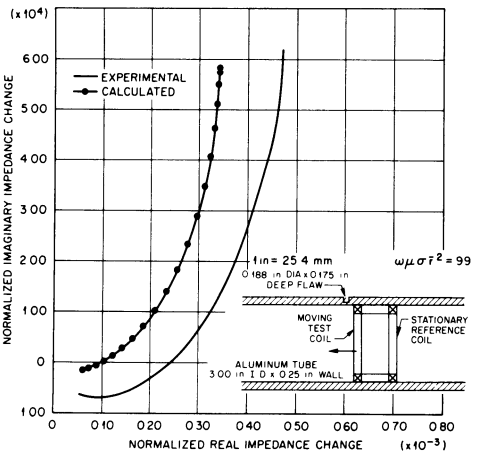

Fig. 4. Boreside scan of absolute coil past a flaw on the outer surface of tube.

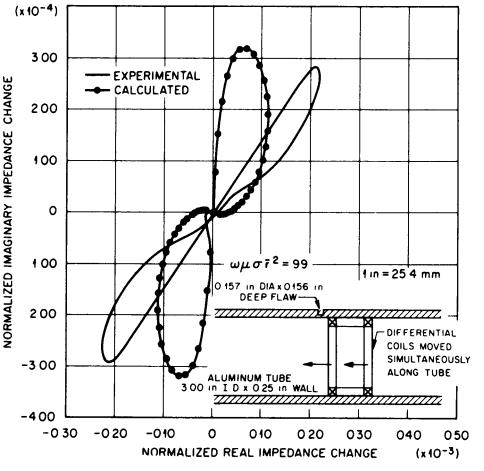

Fig. 5. Boreside scan of differential coils past a flaw on the outer surface of tube.

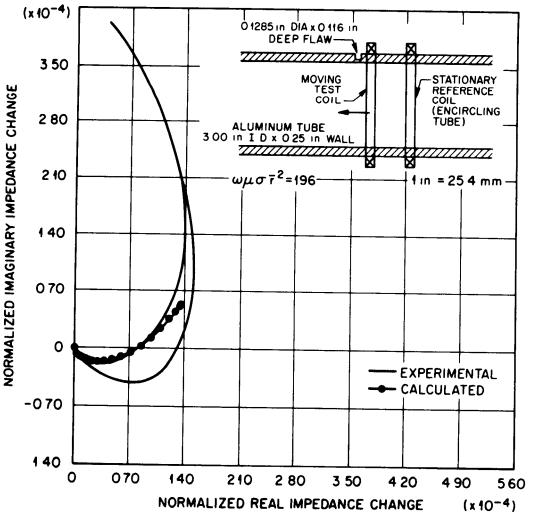

Fig. 6. Scan of absolute encircling coil past a flaw on the outer surface of tube.

PULSED EDDY CURRENTS

We have also made calculations for the determination of multiple properties by the use of pulsed eddy currents, using Fourier synthesis of multiple fixed frequencies to form pulses of various shapes. These results agree very well with experimental measurements and enable us to determine other properties, such as sample thickness, as well as the flaw size and depth. The fitting of the various properties was done using our polynomial expansion method.[5]

FLAW INVERSION THEORY

The integral formulas that we developed for calculating the impedance changes produced in an eddy-current coil by defects of various sizes at various locations are well known, well verified, and widely used. By using the orthogonality of the Bessel functions in the formulas, we can invert the formulas to calculate the size and location of defects from an integral of impedance changes measured over a range of locations.

Explicitly, the normalized impedance change Z_{n_d} produced in a coil above a semi-infinite plane conductor by a defect of normalized volume Vol_n located at cylindrical coordinates r,z can be written as

$$Z_{n_d}(r,z) = \frac{-3(\omega\mu\sigma\bar{r}^2)}{2\pi I_{\mathrm{air}}}\mathrm{Vol}_n\left[\int_0^\infty \frac{J(r_2,r_1)J_1(\alpha r)(e^{-\alpha l_1} - e^{-\alpha l_2})\alpha e^{\alpha_1 z}}{\alpha^3(\alpha + \alpha_1)}\, d\alpha\right]^2, \quad (1)$$

where ω is the angular frequency of the eddy currents, $J(r_2,r_1)$ is the integral of $xJ_1(x)$ with respect to x from r_1 to r_2, and the coil is located at $r_1 \leq r \leq r_2$, $l_1 \leq z \leq l_2$ with mean radius $\bar{r} = (r_1 + r_2)/2$ and an air integral I_{air}. The conductor is located at $z = 0$ and has permeability μ, conductivity σ, and a complex parameter $\alpha_1 \leq \sqrt{\alpha^2 + i\omega\mu\sigma\bar{r}^2}$. A more complicated system of conductors or coils would require a more complicated formula, but the essential procedure would be the same. If one takes the square root of both sides of Eq. (1), multiplies the result by $rJ_1(r)\,dr$, and integrates with respect to r from 0 to ∞, the orthogonality of the Bessel functions $J_1(r)$ makes it possible to obtain the following formula via the Fourier-Bessel integral formula:

$$\sqrt{\mathrm{Vol}_n}\, e^{\alpha_1 z} = \sqrt{\frac{2\pi I_{\mathrm{air}}}{3(\omega\mu\sigma\bar{r}^2)}}\,\frac{(1 + \alpha_1)}{J(r_2,r_1)(e^{-l_1} - e^{-l_2})}\int_0^\infty \sqrt{-Z_{n_d}(r,z)}\, rJ_1(r)\, dr\,. \quad (2)$$

This gives the normalized defect volume Vol_n and depth z in terms of the integral of the square root of the normalized impedance changes Z_{n_d} and other known quantities. Since α_1 and Z_{n_d} are complex variables, Eq. (2) provides two real equations and permits solution for Vol_n and z separately. This would be applicable to a small pancake coil against

the inner wall of a thick tube. If we let $\alpha_1 = x + iy$, so that $x = \mathrm{Re}(\alpha_1)$, $y = \mathrm{Im}(\alpha_1)$, and if we let the right side of Eq. (2) equal $CM_0 e^{i\Theta}$, where

$$C = \sqrt{\frac{2\pi I_{\mathrm{air}}}{3(\omega\mu\sigma\bar{r}^2)}} \; \frac{1}{J(r_2, r_1)[\exp(-l_1) - \exp(-l_2)]} ,$$

$$M_0 = \mathrm{Mag}\left[(1 + \alpha_1)\int_0^\infty \sqrt{-Z_{n_d}(r,z)}\; rJ_1(r)\; dr\right] ,$$

$$\Theta = \mathrm{Pha}\left[(1 + \alpha_1)\int_0^\infty \sqrt{-Z_{n_d}(r,z)}\; rJ_1(r)\; dr\right] ,$$

then the defect depth is $z = \Theta/y$ and the normalized defect volume is $\mathrm{Vol}_n = [CM_0 \exp(-x\,\Theta/y)]^2$.

The same procedure can be applied to cylindrical conductors. For a circumferential coil inside a (very thick) cylindrical conductor, the normalized impedance change Z_{n_d} in a coil of length L and mean radius $\bar{r} = (r_1 + r_2)/2$ can be written as an integral involving the modified Bessel functions $I_1(\alpha_1 r)$:

$$Z_{n_d}(r,z) = \frac{-3(\omega\mu\sigma\bar{r}^2)}{2\pi I_{\mathrm{air}}}\,\mathrm{Vol}_n \left[2\int_0^\infty \frac{I(r_2, r_1)}{\pi\alpha^3}\,\frac{K_1(\alpha_1 r)}{F_2(\alpha_1)}\,\sin\left(\frac{\alpha L}{2}\right)\cos(\alpha z)\; d\alpha\right]^2 , \qquad (3)$$

where $F_2(\alpha_1)$ is a function that depends on the conductor configuration. As before, the orthogonality properties of the cosine functions enable one to invert this formula to obtain the normalized defect volume Vol_n and its radial location [implicitly in the Bessel function $I_1(\alpha_1 r)$]:

$$\sqrt{\mathrm{Vol}_n}\; K_1(\alpha_1 r) = \sqrt{\frac{2\pi I_{\mathrm{air}}}{3(\omega\mu\sigma\bar{r}^2)}}\;\frac{F_2(\alpha_1)}{I(r_2, r_1)\sin(L/2)}\int_0^\infty \sqrt{-Z_{n_d}(r,z)}\,\cos(z)\; dz . \qquad (4)$$

As before, this is a complex equation, equivalent to two real equations, so that Vol_n and r can be calculated separately in terms of the integral and known functions on the right-hand side of the equation.

If more complicated configurations of coils and conductors are involved, the same procedures can still be applied; only the functions in the integrals, such as $F_2(\alpha_1)$, become more complicated.

An important motivation for these flaw inversion studies, in addition to the obvious one of obtaining the flaw parameters, is to develop better basic functions for calculating the flaw properties with fewer terms in the polynomial expressions. If a really accurate function could be found for each flaw property, the polynomial could be reduced to a single term, with a dramatic increase in the speed of signal processing and inspection.

REFERENCES

1. C. V. Dodd, W. E. Deeds, and J. W. Luquire, Integral Solutions to Some Eddy-Current Problems, *Int. J. Nondestr. Test.* 1:29–90 (1969).
2. C. C. Cheng, C. V. Dodd, and W. E. Deeds, General Analysis of Probe Coils Near Stratified Conductors, *Int. J. Nondestr. Test.* 3(2):109–30 (1971).
3. C. V. Dodd, C. C. Cheng, and W. E. Deeds, Induction Coils Coaxial with an Arbitrary Number of Cylindrical Conductors, *J. Appl. Phys.* 45(2):638–47 (1974).
4. M. L. Burrows, "A Theory of Eddy-Current Flaw Detection" (Ph.D. Dissertation), University Microfilms, Inc., Ann Arbor, Michigan (1964).
5. W. E. Deeds and C. V. Dodd, Determination of Multiple Properties with Multiple Eddy-Current Measurements, *Int. Advances Nondestr. Test.* 8:317–33 (1981).